Research Square

Preprints are preliminary reports that have not undergone peer review.
They should not be considered conclusive, used to inform clinical practice,
or referenced by the media as validated information.

# Tertiary Lymphoid Structures in the Prognosis and Immunotherapy of Penile Squamous Cell Carcinoma

**Desi Chen**
Jinan University
**Ting Xue**
Sun Yat-sen University Cancer Center
**Jing Li**
Guangzhou Medical University Cancer Hospital
**Xiheng Hu**
Xiangya Hospital Central South University
**Bonan Chen**
Chinese University of Hong Kong
**Yepeng Guo**
Jinan University
**Gaowei Huang**
ShenZhen People's Hospital
**Zhi Xiao**
Southern University of Science and Technology
**Zhenwei Feng**
Jinan University
**Hui Han**
Sun Yat-sen University Cancer Center
**Xueying Li**
The Seventh Affiliated Hospital of Sun Yat-sen University
**Zaishang Li**
li.zaishang@szhospital.com

ShenZhen People's Hospital

**Research Article**

**Keywords:** penile carcinoma, tertiary lymphoid structures, anti-PD-1 antibody therapy, prognosis

**Posted Date:** September 29th, 2026

**DOI:** https://doi.org/10.21203/rs.3.rs-10947156/v1

**License:** This work is licensed under a Creative Commons Attribution 4.0 International License.
Read Full License

**Additional Declarations:** No competing interests reported.

## Abstract

# Background

Tertiary lymphoid structures (TLSs) are key players in the tumor microenvironment, yet their role in penile squamous cell carcinoma (PSCC) is unexplored. This study investigates TLS presence, prognostic value, and correlation with anti-PD-1 efficacy in PSCC.

# Methods

An immune atlas was constructed from transcriptomic data (56 PSCC, 7 normal tissues). TLSs were assessed via HE and multiplex immunohistochemistry in a SYSUCC cohort (n = 156) and an external validation set (n = 107). A four-tier TLS score-related (TSR) classification was established based on TLS density in tumor nest (TN) and tumor periphery (TS). Correlation with immunotherapy was tested in 30 anti-PD-1-treated patients. Pathway enrichment analysis was performed.

# Results

Significant B-cell infiltration was noted in PSCC. TLSs were identified in TN (44.2%) and TS (54.5%). TSR classification revealed distinct prognostic patterns: high TLS scores in both TN and TS (class Ⅳ) correlated with longest progression-free and overall survival (P<.05). Multivariate analysis confirmed high tnTLS (P=.001), high tpTLS (P=.010), and lymph node metastasis (P<.001) as independent prognostic factors. Notably, class IV patients showed a favorable response rate (100% in this exploratory cohort). Androgen response pathway correlated with high TLS scores in both compartments.

# Conclusions

TSR classification, reflecting TLS spatial distribution and abundance, may serve as a potential predictor for prognosis and immunotherapy response, pending further validation in PSCC. Androgen response pathway was identified as a potential correlated pathway in transcriptomic analysis, warranting further functional investigation.

## 1. Introduction

Penile squamous cell carcinoma (PSCC) is a rare malignancy with a relatively low incidence in the general population but demonstrates a higher prevalence in specific developing regions [1]. In 2018, approximately 26,700 newly diagnosed cases of penile cancer were reported worldwide [2]. The 10-year survival rate for early-stage penile cancer is approximately 85%, whereas the 2-year survival rate for advanced disease or distant metastasis is approximately 21% [3]. Despite the implementation of diverse therapeutic approaches, the prognosis for advanced PSCC remains poor. Given the limited efficacy of

conventional therapies, there is a critical need to explore alternative strategies as promising treatment options for PSCC [4].

Numerous studies have consistently supported the critical role of immune cell infiltration within the tumor microenvironment as a reliable predictor of the response to immunotherapy and patient survival outcomes [5–9]. Several studies have elucidated the clinical significance of immune cell subpopulations within the tumor microenvironment [10–12]. Despite advancements in studies, the clinical consequences of additional immune cells infiltrating the tumor microenvironment in PSCC remain unclear, necessitating further investigation.

Tertiary lymphoid structures (TLSs) emerge as structured lymphoid aggregates in inflamed microenvironments closely associated with autoimmune diseases, cancer, and infectious conditions [13–15]. TLSs are crucial in modulating the recruitment and activation of diverse immune cell populations comprising T cells, B cells, and dendritic cells within the localized tumor microenvironment [16–20]. Additionally, TLSs play a critical role in initiating tumor-specific immune responses by enhancing the generation of tumor-specific antibodies and triggering the activation of cytotoxic T lymphocytes [21–23].

The presence and characteristics of TLSs exhibit a positive correlation with favourable clinical outcomes in particular cancer subtypes [24–28]. Additionally, other studies have demonstrated a positive correlation between augmented TLS density and functionality with improved patient prognosis and increased efficacy of immunotherapy [29–31]. Therefore, a comprehensive understanding of the significance of TLSs in tumors facilitates the development of novel therapeutic strategies and improves patient prognosis.

In this study, we aimed to assess the spatial distribution, abundance, and composition of TLSs in patients with PSCC to reveal the divergent prognostic roles of TLSs in the tumor nest and periphery.

## 2. Materials and Methods

## 2.1. Patients and samples

This study included 293 patients with PSCC from three cohorts (cohorts 1, 2, and 3). Cohort 1 was the primary cohort of 156 patients with PSCCs who underwent curative surgery at Sun Yat-sen University Cancer Center from September 2008 to December 2020. Cohort 2 was used for validation and comprised 107 patients with PSCC from Affiliated Cancer Hospital and Institute of Guangzhou Medical University, Xiangya Hospital and Shenzhen People's Hospital from March 2011 to February 2022. Patients with a medical history of autoimmune diseases and those who had received immunosuppressive chemotherapy or molecular-targeted therapies were excluded.

Cohort 3 comprised 30 patients with PSCC who received anti-programmed cell death protein 1 (PD-1) antibody treatment at Sun Yat-sen University Cancer Center from June 2014 to March 2021. According

to the Response Evaluation Criteria in Solid Tumors (RECIST), version 1, immune checkpoint inhibitor therapy responses were assessed as the best overall response.

Clinical characteristics were extracted from medical records, including age, smoking history, phimosis history, human papillomavirus (HPV) status, clinical stage, histological grade, perioperative treatment details, date of disease progression, and survival status. Tumor staging was determined according to the 8th American Joint Committee on Cancer (AJCC) of tumor-node-metastasis (TNM) classification staging system. This study was approved by our institutional review board.

## 2.2. Estimation of the immune microenvironment composition

Transcriptomic data from 56 PSCC tissues in Cohort 1 and 7 normal tissues were normalized and transformed after quality control and mapping of raw sequencing data. The immune microenvironment (IME) of each sample was assessed using the MCP-counter tool, which provides abundance scores for immune cells (T cells, CD8 + T cells, cytotoxic lymphocytes, natural killer [NK] cells, monocytic lineage, myeloid dendritic cells, and cancer-associated fibroblasts). The cell composition score is based on analyzing specific transcriptomic markers stably and precisely expressed in a unique cell population by TIMER 2.0 [32]

## 2.3. Gene expression profiling

Estimation of the presence of TLSs could be evaluated by gene expression signature, as previously described, including CCL2, CCL3, CCL4, CCL5, CCL8, CCL18, CCL19, CCL21, CXCL9, CXCL10, CXCL11, and CXCL12 et al [33]. The gene expression profile data obtained from the PSCC samples was consistent with that of the sample collected in the preceding step. The differential expression levels of chemokines were determined by analyzing the transcription levels present in the sample.

## 2.4. Pathological evaluation of TLS

TLSs were morphologically assessed on haematoxylin and eosin (H&E)-stained slides and scanned into whole-slide images (WSIs) using Axio Scan (Zeiss). All WSIs were divided into tumor nest (tumor tissue) and periphery (adjacent nontumor tissue) separately. The tumor periphery refers to the region surrounding and close to the tumor nest (Fig. 1A) [34, 35]. The abundance of TLS within the tumor nest and periphery was scored as 0, 1, 2, and 3 as following [36]: (A) a score of 0 indicates no TLS, (B) a score of 1 indicates a tumor with one or two TLS, (C) a score of 2 represents at least three TLS in the tumor but does not meet score 3 criteria, and (D) a score of 3 represents a large number of TLS distributed throughout the tumor region and converging with each other (Fig. 1B). Two experienced pathologists blinded to the clinical data assessed each slide independently. In case of inconsistent diagnostic scores, consensus was reached through joint reading and discussion.

## 2.5. mIHC and data analysis

PANO 5-plex IHC kit (Panovue, Beijing, China) was used in multiplex immunofluorescence staining. Nuclei were stained with 4'-6'-diamidino-2-phenylindole (DAPI, SIGMA-ALDRICH, D9542) after labelling all the human antigens. Immune markers assessed included CD21, CD8, CD20, and CD4; tumor cells were identified with pan-cytokeratin (Pan-CK) antibodies, and nuclei were stained with DAPI (PerkinElmer). Then, slides were incubated with corresponding HRP-conjugated secondary antibodies and fluorescent dyes in the following order: PPD570, PPD480, PPD520, PPD650, and PPD780 (PerkinElmer). The stained slides were scanned with a Mantra System (PerkinElmer), and images were analysed using InForm image analysis software (V.2.4.2, PerkinElmer). Subsequently, the slides were scanned and imaged using the Mantra Quantitative Pathology Workstation (PerkinElmer).

## 2.6. Statistical analysis

Statistical analysis was performed using SPSS software V.23.0. Categorical variables were assessed with the chi-square or Fisher's exact test. Continuous variables were evaluated using Student's t-test or Mann-Whitney U test and summarized as the mean with standard deviation or median and interquartile range.

Progression-free survival (PFS) was defined as the time from initiating treatment to the date of disease progression or death from any cause. Overall survival (OS) was defined as the time from initiating treatment to death for any reason. PFS and OS were estimated using the Kaplan-Meier method. The log-rank test was used for subgroup comparisons, and the Cox proportional hazards regression model was used for computing the hazard ratio (HR) and univariate/multivariate analyses. The multivariate Cox regression model included variables with a *P*-value < .05 in the univariate analyses. A two-sided *P* value < .05 was considered statistically significant.

# 3. Results

### 3.1. Active immune microenvironment (IME) composition of PSCC

The MCP counter was used to evaluate the immune cell composition in 56 PSCC tissues and 7 normal tissues to assess the IME composition using gene expression profiles. The heatmap showed significant discrepancies in the composition of IME between PSCC and normal tissues (Figure 1A). Within the PSCC group, most samples displayed enrichment in monocytic lineage, NK cells, CD8+ T-cells, cytotoxic lymphocytes, myeloid dendritic cells, T cells, B cells, and cancer-associated fibroblast (Figure 2A). It is worth mentioning that a significant infiltration of B cells was observed in many cases, indicating the possible existence of TLSs in PSCC (Figure 3). To conduct a more comprehensive investigation into the impact of TLSs on PSCC, we analysed the transcriptomic data of known molecular markers of TLS formation, including CCL2, CCL3, CCL4, CCL8, CXCL9 et al [37,38]. These markers were all upregulated in tumor tissue compared to normal tissue (all $p<0.05$, Figure 2B). The collective findings from the investigations above showed a significant infiltration of immune cells in the tumor microenvironment, suggesting the likely existence of TLSs within the immune microenvironment of PSCC.

Enhance, we further confirmed the presence of TLSs in PSCC by H&E staining (Figure 1). We classified them into low-tnTLS (score 0 and 1 in tumor nest) and high-tnTLS (score 2 and 3 in tumor nest), low-tpTLS (score 0 and 1 in tumor periphery), and high-tpTLS (score 2 and 3 in tumor periphery). Out of the 156 patients in cohort 1, 87 individuals (55.8%) exhibited low-tnTLS, while high-tnTLS was observed in 69 patients (44.2%). Additionally, 71 patients (44.5%) displayed low tpTLS, whereas high tpTLS was present in 85 individuals (54.5%).

To confirm the tumor immune environment of TLSs in PSCC, we performed mIHC staining on 20 PSCC samples from cohort 1 (Figure 2C). The results showed that TLSs were frequently observed as clusters of CD20+ B-cell zones, CD21 follicular dendritic cells, CD4+ T cells, and CD8+ T-cells in the tumor nest and periphery. Noteworthy, B cells organized in the follicular architecture were the prevailing constituents of TLSs. The low-tnTLS group and low-tpTLS group exhibited lower CD4+ T cells, CD8+ T cells, CD20+ B cells, and CD21 follicular dendritic cells than the high-tnTLS group and high-tpTLS group (Figure 4, all $p<0.01$).

3.2. Relationship between TLSs expression and clinicopathological and prognosis of PSCC

We investigated the correlation between the various TLS groups and the clinicopathological characteristics of PSCC in cohort 1, which comprised individuals with a median (IQR) age of 54 (26–86) years. Until September 2023, the median follow-up time was 51.367 (38.905-63.829) months. Compared with high tnTLS, low tnTLS was significantly associated with advanced T stage(≧T2) 66.7% vs. 33.3%, $p=0.008$), lymph node metastasis (LNM) (69.4% vs. 30.6%, $p=0.006$), and advanced clinical stage III-IV) (70.8% vs. 29.2%, $p=0.001$). Additionally, low tpTLS was significantly associated with LNM (69.4% vs. 30.6%, $p<0.001$), distant metastasis (100% vs. 0%, $p=0.041$), and advanced clinical stage (III-IV) (70.8% vs. 29.2%, $p<0.001$) compared with high tsTLS (Table S1).

Figure 5 presents the survival curves of PFS and OS. The high-tnTLS group (median PFS: not reached [NR]; median OS: NR) showed significantly longer PFS and OS than the low-tnTLS group (median PFS: 43.867, 95%CI: 24.213-NR; median OS: NR) (PFS: HR= 0.202, 95%CI: 0.095-0.429, $p<0.001$; OS: HR= 0.057, 95%CI: 0.014-0.238, $p<0.001$) (Figure 5A). The high-tpTLS group (median PFS: NR; median OS: NR) was positively associated with longer PFS and OS compared with the low-tpTLS group (median PFS: 13.233, 95%CI: 4.830-21.637; median OS: 23.833, 95%CI: 14.441-33.225) (PFS: HR= 0.113, 95%CI: 0.057-0.222; OS: HR= 0.123, 95%CI: 0.058-0.262, $p<0.001$) (Figure 5B).

Univariate analysis revealed that PFS was significantly associated with HPV status, T stage, LNM, M stage, histological grade, tnTLS group, and tpTLS group ($p<0.05$, Table 1). Multivariate analysis showed that PFS was significantly associated with high tnTLS (HR=0.352, 95%CI: 0.158-0.786, $p=0.011$), high tpTLS (HR=0.243 95%CI: 0.115-0.511, $p<0.001$), and LNM (HR=8.521, 95%CI: 3.601-20.163, $p<0.001$) (Table 1)

Univariate analysis revealed that OS was significantly associated with HPV status, T stage, LNM, M stage, histological grade, tnTLS, and tpTLS ($p<0.05$, Table 1). Multivariate analysis showed that OS was

significantly associated with high tnTLS (HR=0.080, 95%CI: 0.019-0.344, p=0.001), high tpTLS (HR=0.343, 95%CI: 0.152-0.775, p=0.010), and LNM (HR=10.666, 95% CI: 3.923-29.001, p<0.001) (Table 1).

To further investigate the difference between different TLS groups, we performed RNA-seq in 14 low-tnTLS and 23 high-tnTLS cases and 18 low-tpTLS and 19 high-tpTLS cases from cohort 1.

We identified 37 downregulated and 45 upregulated genes in high tnTLS cases than low tnTLS (p<.05) (Figure 5C). Those genes were subjected to GSVA pathway enrichment analysis. The analysis demonstrated that these differential genes (DEGs) were mainly involved in androgen response, fatty acid metabolism, apoptosis, protein secretion, adipogenesis, and coagulation (Figure 5D). For the tpTLS group, we identified 105 downregulated and 59 upregulated genes in high cases than low cases (P<.05) (Figure 5E). Those genes were subjected to GSVA pathway enrichment analysis. The analysis demonstrated that these DEGs were mainly involved in apoptosis androgen response, IL2-STAT5-signaling, complement, protein secretion, epithelial-mesenchymal transition, IL6-JAK-STAT3-signaling, and coagulation (Figure 5F). It is important to note that these findings are derived solely from gene set variation analysis (GSVA) of bulk RNA-sequencing data. Whether the androgen signaling pathway directly promotes or inhibits TLS formation in PSCC remains unknown and requires rigorous in vitro and in vivo functional studies.

3.3. An immune class combining the tnTLS and tsTLS

The GSVA showed that the high tnTLS and high tpTLS groups might play an important role in anti-tumor function. So, we combined the two groups to further investigate the synergistic roles of tnTLS and tpTLS in predicting PSCC prognosis. Based on these two protective factors, patients with PSCC were categorized into four TLS-related classes (TSR classes): class I (low-tnTLS and low-tpTLS), class II (low-tnTLS and high-tpTLS), class III (high-tnTLS and low-tpTLS), and class IV (high-tnTLS and high-tpTLS), representing the distribution and abundance of TLSs.

Patients with PSCC in the four TSR classes showed significant differences in PFS and OS (all p<0.05, Figure 6A, 6B). Patients in the TSR class IV cohort demonstrated markedly improved PFS and OS outcomes in comparison to patients in the remaining cohorts, and TSR class IV was at a significantly lowest risk (p<0.05) (Figure 6A, 6B). The results indicate that varying groups exhibited distinct prognoses.

To verify the diagnostic accuracy of the TSR class in predicting the PFS and OS of patients with PSCC, the C-indices of the tnTLS, tpTLS, and TSR classes were assessed. The C-index of the TSR class for PFS prediction was 0.768 (95% CI, 0.719–0.817), which was higher than that of tnTLS (0.662) (95% CI, 0.605–0.719) and tpTLS (0.642) (95% CI, 0.592–0.791). For OS prediction, the C-index of the TSR class was 0.768 (95% CI, 0.715–0.820), which was higher than that of tnTLS (0.618) (95% CI, 0.575–0.761) and tpTLS (0.642) (95% CI, 0.592–0.792).

Additionally, we verified the distinct prognoses of the four classes in an external cohort (cohort 2). External cohort data also indicate that the TSR class significantly predicts survival outcomes for PFS and OS. (Figure 6C, 6D)

3.4. Predictive value of TSR class for treatment response and prognosis of anti-PD-1 antibody therapy in PSCC patients

To further validate the role of TLS in predicting immunotherapeutic benefits, we examined the predictive values of the TSR class in a different cohort of PSCC patients treated with anti-PD-1 antibody monotherapy (cohort 3).

TSR class was significantly correlated with the clinical response to anti-PD-1 antibody therapy ($p<0.05$). Regarding the CR/PR patients, the distributions of the four classes were as follows: 50%, 66.7%, 80.0%, and 100.0% for classes I, II, III, and IV, respectively (Figure 7A). Survival analysis in this cohort revealed that class IV was associated with significantly better PFS and OS (PFS: HR=0.265, 95% CI=0.028–0.413, p=0.044; OS: HR=0.312, 95% CI=0.039–0.451, p=0.002) (Figure 7B, 7C). These results confirmed that the TLS-related score might be a new predictor of PD-1 inhibitor therapy response in PSCC.

# 4. Discussion

To our knowledge, this study recruited the largest cohort of patients that analysed the TLS in PSCC. We examined TLS expression and its association with patient characteristics and prognosis. High TLS expression in the tumor nest and periphery correlated with OS or PFS benefits. We established a TSR class (four classes) based on TLS expression in the tumor nest and periphery. The four TSR classes identified in this study exhibited different immune infiltrates, which could offer valuable insights into predicting the clinical response to anti-PD-1 antibodies and patient survival. To the best of our knowledge, this is the first study to illustrate the clinical significance of TLSs in predicting the prognosis and effectiveness of anti-PD-1 antibody treatment in a large cohort of patients with PSCC.

Vassallo et al. verified the infiltration of CD3, CD4, CD8, CD20, CD68, CD138, and FOXP3 by immunohistochemical in PSCC [10]. In line with the findings of Vassallo, we also found a higher level of immune cell infiltration in PSCC compared to normal tissues by RNA-sequencing. Besides this, we also found the up-regulation of chemokines, which suggests the involvement of TLS neogenesis [39–41]. These findings suggest the presence of TLSs in PSCC, and the high infiltration of B cells indicates a potential role of adaptive immune response in antitumor immunity.

The formation of TLS has the potential to impede tumor growth through the upregulation of tumor antigen-specific or activated cytotoxic lymphocytes, [40] thereby enhancing the anti-tumor immune response and conferring a favourable prognostic outcome [24, 42–45]. In our study, TLS in the tumor nest and periphery were associated with a favourable clinical outcome in patients. We further compared the differentially expressed genes between different tnTLS and tpTLS groups, and the results showed that high TLS in both the tumor nest and the tumor periphery contributed to the formation and shaping of

the immune context in an anti-tumor direction. Diverse distribution patterns of TLS contribute to forming distinct microanatomical sites, facilitating anti-tumor immune responses [42, 46–50].

To further understand the role of TLS in PSCC, we integrate the TLS expression both in intratumor and peritumor. A TSR class was established to stratify patients into four distinct subclasses with significantly varied prognoses. Class IV denotes patients with significant tumor nest and periphery infiltration. Class I represents the opposite combination, with the least effective anti-tumor response and the poorest prognosis. Immune class II and III represent patients with distribution and abundance of TLSs in tumor nest or tumor periphery. This classification based on immune-related factors has been granted clinical validation for practical application in colorectal cancer and intrahepatic cholangiocarcinoma [36, 51–54]. Similarly, our TSR class has demonstrated a robust and reliable prognostic value for PSCC patients in internal and external cohorts, highlighting our immune classification system's exceptional reliability and discriminatory ability.

To further confirm the practicality of the TSR class, a cohort of 30 patients who underwent PD-1 blockade therapy was included to assess its predictive capability for immunotherapy response. The results indicated that the TSR class could be an indicator for PD-1 blockade application in PSCC.

This study has several limitations. First, the predictive power of the TRS class for immunotherapy response and its prognostic value as a biomarker in PSCC should be further validated through a more extensive cohort study. Second, the mechanisms underlying TLS formation and distribution in PSCC remain unclear. Third, investigating the dynamic alterations in tumor-infiltrating lymphocyte composition within tumor-associated TLS during tumor progression and exploring the potential modulatory effects of emerging clinical interventions on these alterations holds significant implications for future scientific inquiry. Fourth, the immunotherapy cohort (Cohort 3) comprised a relatively small sample size (n = 30). Therefore, the observed predictive value of the TSR class for anti-PD-1 efficacy is exploratory and requires confirmation in larger prospective studies.

## 5. Conclusions

In summary, we demonstrated that the spatial arrangement and abundance of TLSs are significantly correlated with prognosis and present a novel TSR classification for predicting survival in PSCC patients.

## Declarations

# Ethics approval and consent to participate

This study was approved by the institutional ethics committees of Shenzhen People’s Hospital, and the requirement for informed consent was waived owing to its retrospective nature. This study followed the Strengthening the Reporting of Observational Studies in Epidemiology (STROBE) reporting guideline.

# Consent for publication

All authors agreed on submitting and publishing this manuscript. This article is the authors' original work, and has neither been received for publication, nor under consideration for publication elsewhere.

# Competing interests

The authors declare no conflicts of interest.

# Funding

This study was supported by Guangdong Province Nature Foundation of China Project (No. 2022A1515012200 to Li ZS), Guangdong Basic and Applied Basic Research Foundation (No. 2021A1515220182, No.2022A1515012321 to Hui Han), Shenzhen Science and Technology Program (RCYX20221008093032008 to Li ZS).

# Author Contribution

D.C. curated the data, performed formal analysis and investigation, created visualizations, and wrote the original draft. T.X. contributed to conceptualization and methodology, administered and supervised the project, provided resources, and reviewed and edited the manuscript. J.L. curated the data, conducted the investigation, and provided resources. X.H. curated the data, conducted the investigation, and provided resources. B.C. curated the data, conducted the investigation, and provided resources. Y.G. curated the data, conducted the investigation, and created visualizations. G.H. performed formal analysis and validation and created visualizations. X.Z. curated the data. Z.F. curated the data. H.H. contributed to conceptualization and methodology, acquired funding, and administered and supervised the project. X.L. contributed to conceptualization and methodology, administered and supervised the project, provided resources, and reviewed and edited the manuscript. Z.L. contributed to conceptualization and methodology, acquired funding, administered and supervised the project, provided resources, performed validation, and reviewed and edited the manuscript. All authors reviewed and approved the final manuscript.

# Acknowledgement

Our special acknowledgments to Wiley Editing Services for English language editing.

# Availability of data and material

All data relevant to the study are included in the article.

## Glossary

AJCC: American Joint Committee on Cancer;

H&E: hematoxylin and eosin;

HPV: human papillomavirus;

IHC: immunohistochemical;

IME: immune microenvironment;

LNM: lymph node metastasis;

mIHC: multiplex immunohistochemical staining;

NK: natural killer;

OS: overall survival;

PFS: progression-free survival;

PSCC: penile squamous cell carcinoma;

TLSs: tertiary lymphoid structures;

TN: tumor nest;

TNM: tumor-node-metastasis;

TS: tumor periphery;

## Tables

Tables 1 & 2 are available in the Supplementary Files section.

## References


1. Pow-Sang MR, Ferreira U, Pow-Sang JM, Nardi AC, Destefano V. Epidemiology and Natural History of Penile Cancer. Urology. 2010;76(2):S2–6. 10.1016/j.urology.2010.03.003.
2. Sung H, Ferlay J, Siegel RL, et al. Global Cancer Statistics 2020: GLOBOCAN Estimates of Incidence and Mortality Worldwide for 36 Cancers in 185 Countries. CA Cancer J Clin. 2021;71(3):209–49. 10.3322/caac.21660.

3. Graafland NM, Verhoeven RHA, Coebergh JW, Horenblas S. Incidence trends and survival of penile squamous cell carcinoma in the Netherlands. Int J Cancer. 2011;128(2):426–32. 10.1002/ijc.25355.
4. Tang Y, Hu X, Wu K, Li X. Immune landscape and immunotherapy for penile cancer. Front Immunol. 2022;13:1055235. 10.3389/fimmu.2022.1055235.
5. Bao J, Betzler AC, Hess J, Brunner C. Exploring the dual role of B cells in solid tumors: implications for head and neck squamous cell carcinoma. Front Immunol. 2023;14:1233085. 10.3389/fimmu.2023.1233085.
6. Capodanno Y, Hirth M. Targeting the Cancer–Neuronal Crosstalk in the Pancreatic Cancer Microenvironment. Int J Mol Sci. 2023;24(19):14989. 10.3390/ijms241914989.
7. Castillo-Peña A, Molina-Pinelo S. Landscape of tumor and immune system cells-derived exosomes in lung cancer: mediators of antitumor immunity regulation. Front Immunol. 2023;14:1279495. 10.3389/fimmu.2023.1279495.
8. Gorenšek R, Kresnik M, Takač I, Rojko T, Sobočan M. Advances in Tumour-Infiltrating Lymphocytes for Triple-Negative Breast Cancer Management. Breast Cancer Targets Ther. 2023;15:773–83. 10.2147/BCTT.S399157.
9. Cai W, Jing M, Gu Y, et al. Tumor microenvironment features decipher the outperformance of neoadjuvant immunochemotherapy over chemotherapy in resectable non-small cell lung cancer. Front Immunol. 2022;13:984666. 10.3389/fimmu.2022.984666.
10. Vassallo J, Rodrigues AFF, Campos AHJFM, et al. Pathologic and imunohistochemical characterization of tumoral inflammatory cell infiltrate in invasive penile squamous cell carcinomas: Fox-P3 expression is an independent predictor of recurrence. Tumor Biol. 2015;36(4):2509–16. 10.1007/s13277-014-2864-2.
11. Cocks M, Taheri D, Ball MW, et al. Immune-checkpoint status in penile squamous cell carcinoma: a North American cohort. Hum Pathol. 2017;59:55–61. 10.1016/j.humpath.2016.09.003.
12. Ahmed ME, Falasiri S, Hajiran A, Chahoud J, Spiess PE. The Immune Microenvironment in Penile Cancer and Rationale for Immunotherapy. J Clin Med. 2020;9(10):3334. 10.3390/jcm9103334.
13. Esparcia-Pinedo L, Romero-Laorden N, Alfranca A. Tertiary lymphoid structures and B lymphocytes: a promising therapeutic strategy to fight cancer. Front Immunol. 2023;14:1231315. 10.3389/fimmu.2023.1231315.
14. Zhang NN, Qu FJ, Liu H, et al. Prognostic impact of tertiary lymphoid structures in breast cancer prognosis: a systematic review and meta-analysis. Cancer Cell Int. 2021;21(1):536. 10.1186/s12935-021-02242-x.
15. Goc J, Fridman WH, Hammond SA, Sautès-Fridman C, Dieu-Nosjean MC. Tertiary lymphoid structures in human lung cancers, a new driver of antitumor immune responses. OncoImmunology. 2014;3(6):e28976. 10.4161/onci.28976.
16. Fridman WH, Meylan M, Pupier G, Calvez A, Hernandez I, Sautès-Fridman C. Tertiary lymphoid structures and B cells: An intratumoral immunity cycle. Immunity. 2023;56(10):2254–69. 10.1016/j.immuni.2023.08.009.

17. Pagès F, Mlecnik B, Marliot F, et al. International validation of the consensus Immunoscore for the classification of colon cancer: a prognostic and accuracy study. Lancet. 2018;391(10135):2128–39. 10.1016/S0140-6736(18)30789-X.
18. Roulleaux Dugage M, Nassif EF, Italiano A, Bahleda R. Improving Immunotherapy Efficacy in Soft-Tissue Sarcomas: A Biomarker Driven and Histotype Tailored Review. Front Immunol. 2021;12:775761. 10.3389/fimmu.2021.775761.
19. Shen C, Zhang DL, Cheng XL, Zhang WC, Zhao JJ. Urological Tumor: A Narrative Review of Tertiary Lymphatic Structures. Urol Int. 2023;107(9):841–7. 10.1159/000532127.
20. Moyron-Quiroz JE, Rangel-Moreno J, Kusser K, et al. Role of inducible bronchus associated lymphoid tissue (iBALT) in respiratory immunity. Nat Med. 2004;10(9):927–34. 10.1038/nm1091.
21. Buckley CD, Barone F, Nayar S, Bénézech C, Caamaño J. Stromal Cells in Chronic Inflammation and Tertiary Lymphoid Organ Formation. Annu Rev Immunol. 2015;33(1):715–45. 10.1146/annurev-immunol-032713-120252.
22. Sautès-Fridman C, Petitprez F, Calderaro J, Fridman WH. Tertiary lymphoid structures in the era of cancer immunotherapy. Nat Rev Cancer. 2019;19(6):307–25. 10.1038/s41568-019-0144-6.
23. Sarti Kinker G, Da Silva Medina T. Tertiary lymphoid structures as hubs of antitumour immunity. Nat Rev Cancer. 2023;23(12):803–803. 10.1038/s41568-023-00626-x.
24. Karjula T, Niskakangas A, Mustonen O, et al. Tertiary lymphoid structures in pulmonary metastases of microsatellite stable colorectal cancer. Virchows Arch. 2023;483(1):21–32. 10.1007/s00428-023-03577-8.
25. Liu J, Yue J, Wang K, et al. Tertiary Lymphoid Structures Are Related to Inflammatory Progression and Bone Loss in Human Apical Periodontitis. J Endod. 2023;49(9):1138–44. 10.1016/j.joen.2023.06.006.
26. Lu H, Lou H, Wengert G, et al. Tumor and local lymphoid tissue interaction determines prognosis in high-grade serous ovarian cancer. Cell Rep Med. 2023;4(7):101092. 10.1016/j.xcrm.2023.101092.
27. Mao Y, Wang X, Xi L, et al. Prediction values of tertiary lymphoid structures in the prognosis of patients with left- and right-sided colon cancer: a multicenter propensity score-matched study. Int J Surg. 2023;109(8):2344–58. 10.1097/JS9.0000000000000483.
28. Yu A, Cao M, Zhang K, et al. The prognostic value of the tertiary lymphoid structure in gastrointestinal cancers. Front Immunol. 2023;14:1256355. 10.3389/fimmu.2023.1256355.
29. Komura K, Tokushige S, Ishida M, et al. Tertiary lymphoid structure and neutrophil–lymphocyte ratio coordinately predict outcome of pembrolizumab. Cancer Sci. 2023;114(12):4622–31. 10.1111/cas.15976.
30. Nakamura S, Ohuchida K, Hayashi M, et al. Tertiary lymphoid structures correlate with enhancement of antitumor immunity in esophageal squamous cell carcinoma. Br J Cancer. 2023;129(8):1314–26. 10.1038/s41416-023-02396-7.
31. Zou X, Guan C, Gao J, Shi W, Cui Y, Zhong X. Tertiary lymphoid structures in pancreatic cancer: a new target for immunotherapy. Front Immunol. 2023;14:1222719. 10.3389/fimmu.2023.1222719.

32. Li T, Fu J, Zeng Z, et al. TIMER2.0 for analysis of tumor-infiltrating immune cells. Nucleic Acids Res. 2020;48(W1):W509–14. 10.1093/nar/gkaa407.
33. Oba M, Nakanishi Y, Amano T, et al. Stratification of Postoperative Prognosis by Invasive Tumor Thickness in Perihilar Cholangiocarcinoma. Ann Surg Oncol. 2021;28(4):2001–9. 10.1245/s10434-020-09135-9.
34. Germain C, Gnjatic S, Tamzalit F, et al. Presence of B Cells in Tertiary Lymphoid Structures Is Associated with a Protective Immunity in Patients with Lung Cancer. Am J Respir Crit Care Med. 2014;189(7):832–44. 10.1164/rccm.201309-1611OC.
35. Mikami S, Mizuno R, Kondo T, et al. Clinical significance of programmed death-1 and programmed death-ligand 1 expression in the tumor microenvironment of clear cell renal cell carcinoma. Cancer Sci. 2019;110(6):1820–8. 10.1111/cas.14019.
36. Zhang C, Wang XY, Zuo JL, et al. Localization and density of tertiary lymphoid structures associate with molecular subtype and clinical outcome in colorectal cancer liver metastases. J Immunother Cancer. 2023;11(2):e006425. 10.1136/jitc-2022-006425.
37. Cabrita R, Lauss M, Sanna A, et al. Tertiary lymphoid structures improve immunotherapy and survival in melanoma. Nature. 2020;577(7791):561–5. 10.1038/s41586-019-1914-8.
38. Dieu-Nosjean MC, Goc J, Giraldo NA, Sautès-Fridman C, Fridman WH. Tertiary lymphoid structures in cancer and beyond. Trends Immunol. 2014;35(11):571–80. 10.1016/j.it.2014.09.006.
39. Karapetyan L, AbuShukair HM, Li A, et al. Expression of lymphoid structure-associated cytokine/chemokine gene transcripts in tumor and protein in serum are prognostic of melanoma patient outcomes. Front Immunol. 2023;14:1171978. 10.3389/fimmu.2023.1171978.
40. Kroeger DR, Milne K, Nelson BH. Tumor-Infiltrating Plasma Cells Are Associated with Tertiary Lymphoid Structures, Cytolytic T-Cell Responses, and Superior Prognosis in Ovarian Cancer. Clin Cancer Res. 2016;22(12):3005–15. 10.1158/1078-0432.CCR-15-2762.
41. Li H, Ding JY, Zhang MJ, Yu HJ, Sun ZJ. Tertiary lymphoid structures and cytokines interconnections: The implication in cancer immunotherapy. Cancer Lett. 2023;568:216293. 10.1016/j.canlet.2023.216293.
42. Connolly KA, Nader M, Joshi N. Investigating Tumor-Associated Tertiary Lymphoid Structures in Murine Lung Adenocarcinoma. In: Dieu-Nosjean MC, editor. Tertiary Lymphoid Structures. Methods in Molecular Biology. Volume 1845. New York: Springer; 2018. pp. 259–73. 10.1007/978-1-4939-8709-2_15.
43. Federico L, McGrail DJ, Bentebibel SE, et al. Distinct tumor-infiltrating lymphocyte landscapes are associated with clinical outcomes in localized non-small-cell lung cancer. Ann Oncol. 2022;33(1):42–56. 10.1016/j.annonc.2021.09.021.
44. He M, He Q, Cai X, et al. Intratumoral tertiary lymphoid structure (TLS) maturation is influenced by draining lymph nodes of lung cancer. J Immunother Cancer. 2023;11(4):e005539. 10.1136/jitc-2022-005539.

45. Maibach F, Sadozai H, Seyed Jafari SM, Hunger RE, Schenk M. Tumor-Infiltrating Lymphocytes and Their Prognostic Value in Cutaneous Melanoma. Front Immunol. 2020;11:2105. 10.3389/fimmu.2020.02105.
46. Bruchard M, Ghiringhelli F. Deciphering the Roles of Innate Lymphoid Cells in Cancer. Front Immunol. 2019;10:656. 10.3389/fimmu.2019.00656.
47. Germain C, Devi-Marulkar P, Knockaert S, et al. Tertiary Lymphoid Structure-B Cells Narrow Regulatory T Cells Impact in Lung Cancer Patients. Front Immunol. 2021;12:626776. 10.3389/fimmu.2021.626776.
48. Goc J, Germain C, Vo-Bourgais TKD, et al. Dendritic Cells in Tumor-Associated Tertiary Lymphoid Structures Signal a Th1 Cytotoxic Immune Contexture and License the Positive Prognostic Value of Infiltrating CD8 + T Cells. Cancer Res. 2014;74(3):705–15. 10.1158/0008-5472.CAN-13-1342.
49. Rakaee M, Kilvaer TK, Jamaly S, et al. Tertiary lymphoid structure score: a promising approach to refine the TNM staging in resected non-small cell lung cancer. Br J Cancer. 2021;124(10):1680–9. 10.1038/s41416-021-01307-y.
50. Zou J, Zhang Y, Zeng Y, et al. Tertiary Lymphoid Structures: A Potential Biomarker for Anti-Cancer Therapy. Cancers. 2022;14(23):5968. 10.3390/cancers14235968.
51. Ding GY, Ma JQ, Yun JP, et al. Distribution and density of tertiary lymphoid structures predict clinical outcome in intrahepatic cholangiocarcinoma. J Hepatol. 2022;76(3):608–18. 10.1016/j.jhep.2021.10.030.
52. Randall TD, Kern JA. Tertiary Lymphoid Structures Target the Antitumor Immune Response to Lung Cancer. Am J Respir Crit Care Med. 2014;189(7):767–9. 10.1164/rccm.201402-0317ED.
53. Ren F, Xie M, Gao J, et al. Tertiary lymphoid structures in lung adenocarcinoma: characteristics and related factors. Cancer Med. 2022;11(15):2969–77. 10.1002/cam4.4796.
54. Bertucci F, De Nonneville A, Finetti P, Mamessier E. Predictive power of tertiary lymphoid structure signature for neoadjuvant chemotherapy response and immunotherapy benefit in HER2-negative breast cancer. Cancer Commun. 2023;43(8):943–6. 10.1002/cac2.12447.

# Figures

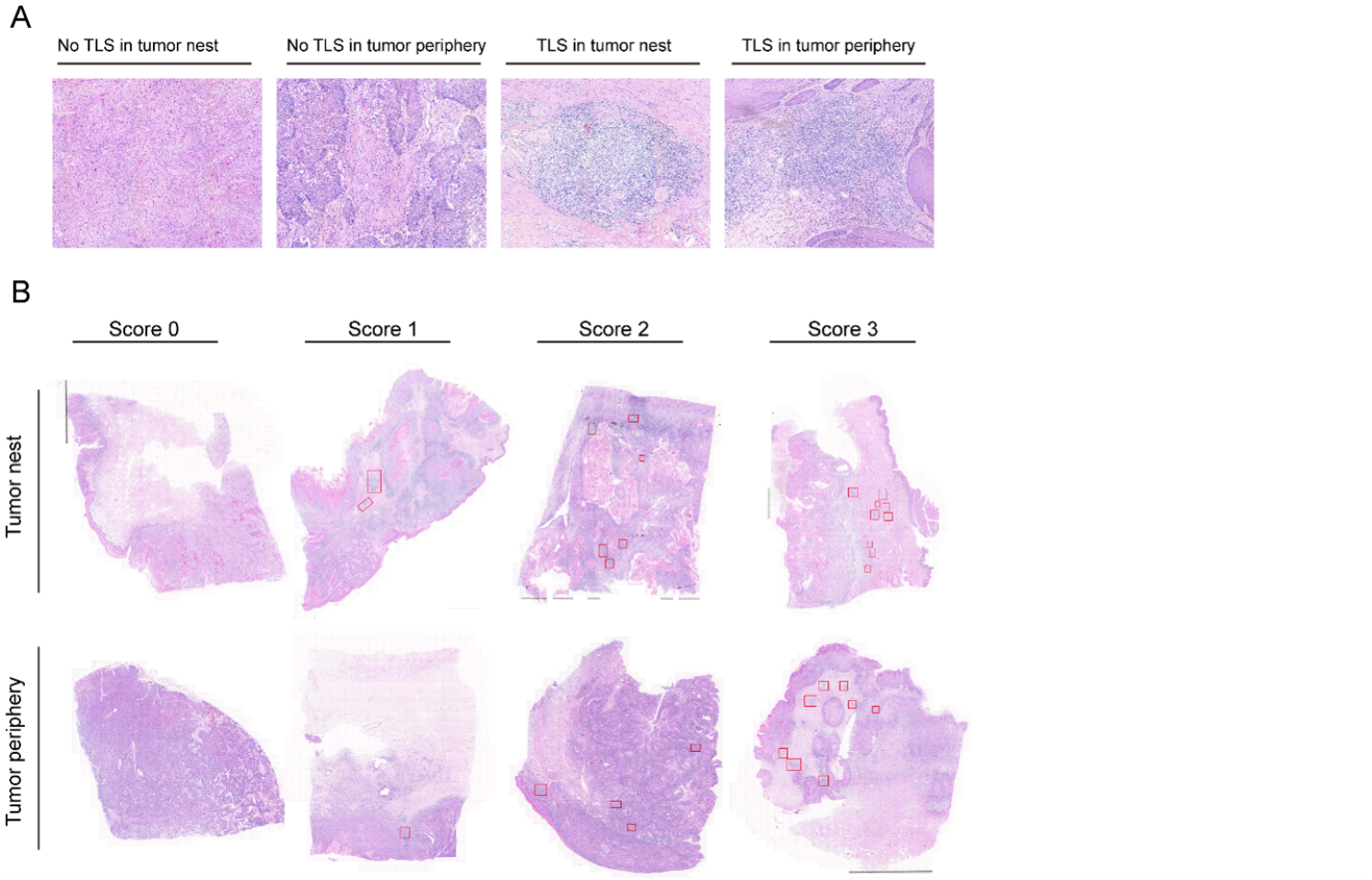


**Figure 1**

Representative whole slide images of H&E staining for TLS scoring system (TN and TP scores). Representative images of TLS in tumor nest and tumor periphery (A). Representative TLS score images in the intratumor and periphery region were shown in (B), and TLS was marked in red.

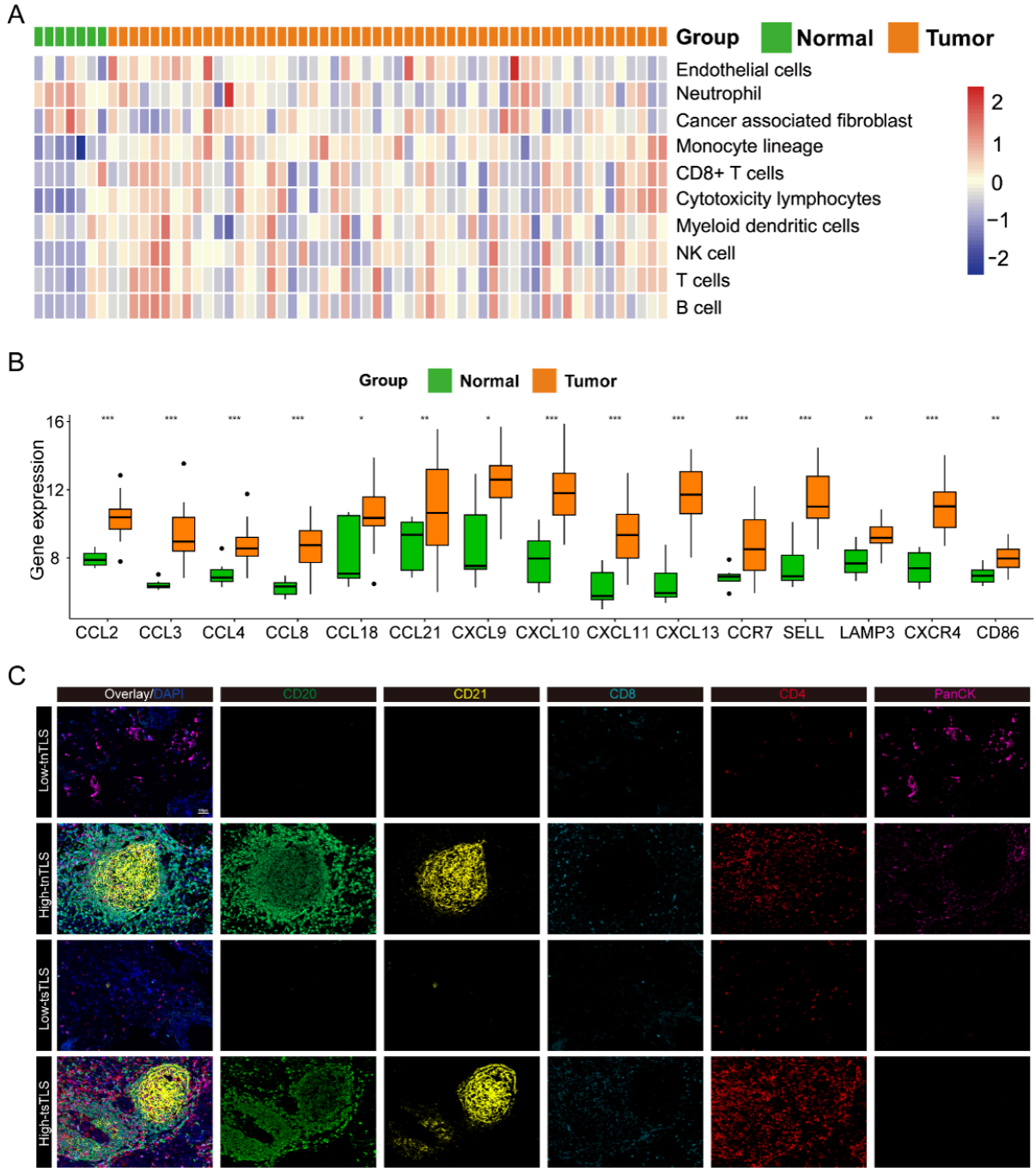


## Figure 2

Immune microenvironment (IME) compositions of PSCC and normal tissues. (A) IME compositions between tumor and normal tissues defined by the MCP-counter. (B) Differential expressions of TLS-related chemokines in tumor and normal groups. (*$P$ < .05, ** $P$ < .01, ***$P$< .001). Comparisons were made using the Mann-Whitney U test. (C) Evaluation of tertiary lymphoid structures (TLSs) using multiplex immunofluorescence in 20 PSCC patients. Representative image of low-tnTLS, high-tnTLS, low-tpTLS, and high-tpTLS, showing B cells (CD20, green), follicular DCs (CD21, yellow), CD8 T cells (CD8, blue), CD4 T cells (CD4, red), panCK (tumor cell, purple). Scale bars = 100 μm.

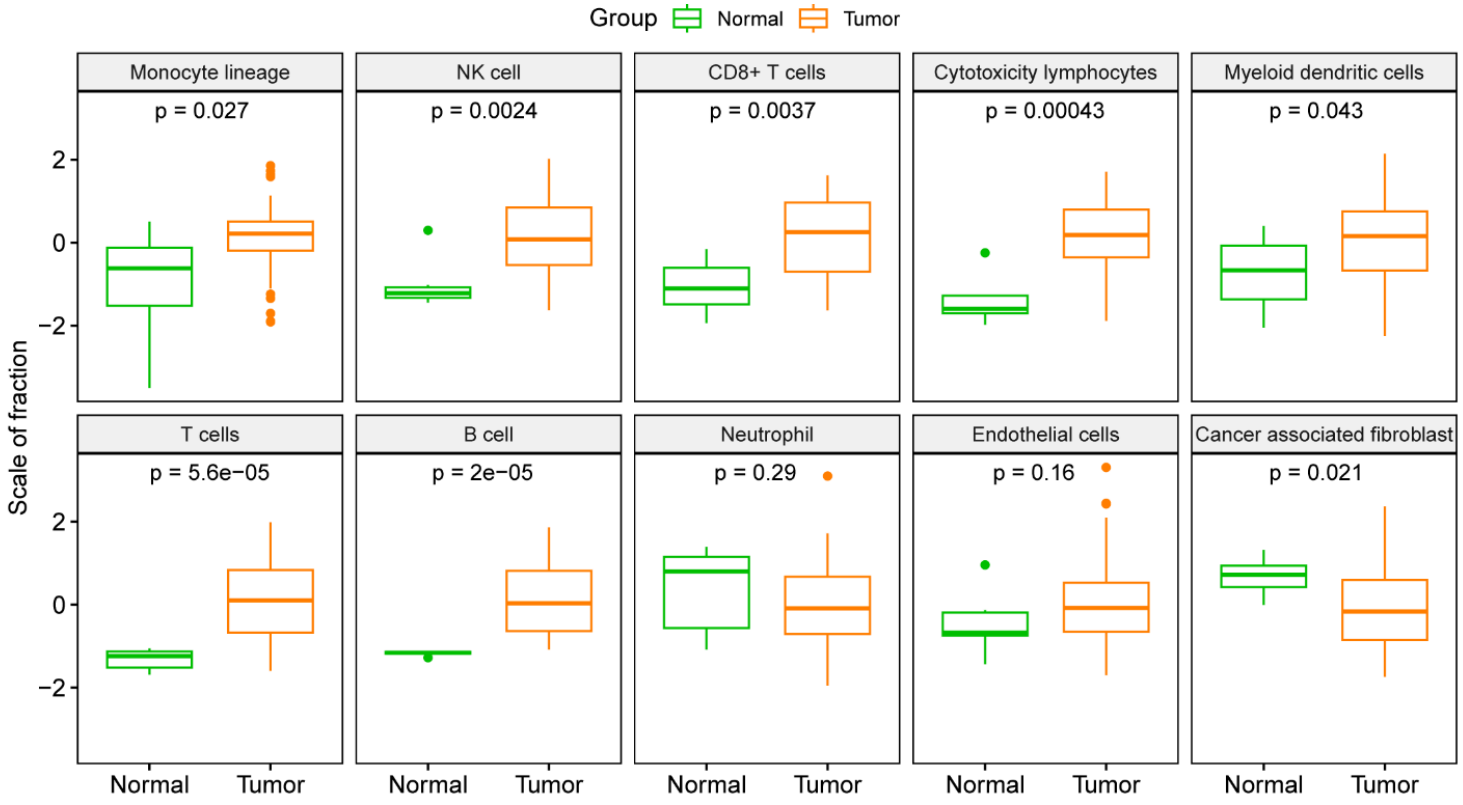


**Figure 3**

The boxplot shows the MCPcounter enrichment scores of immune cell fractions between normal and tumor groups. Comparisons were made by Mann–Whitney U test.

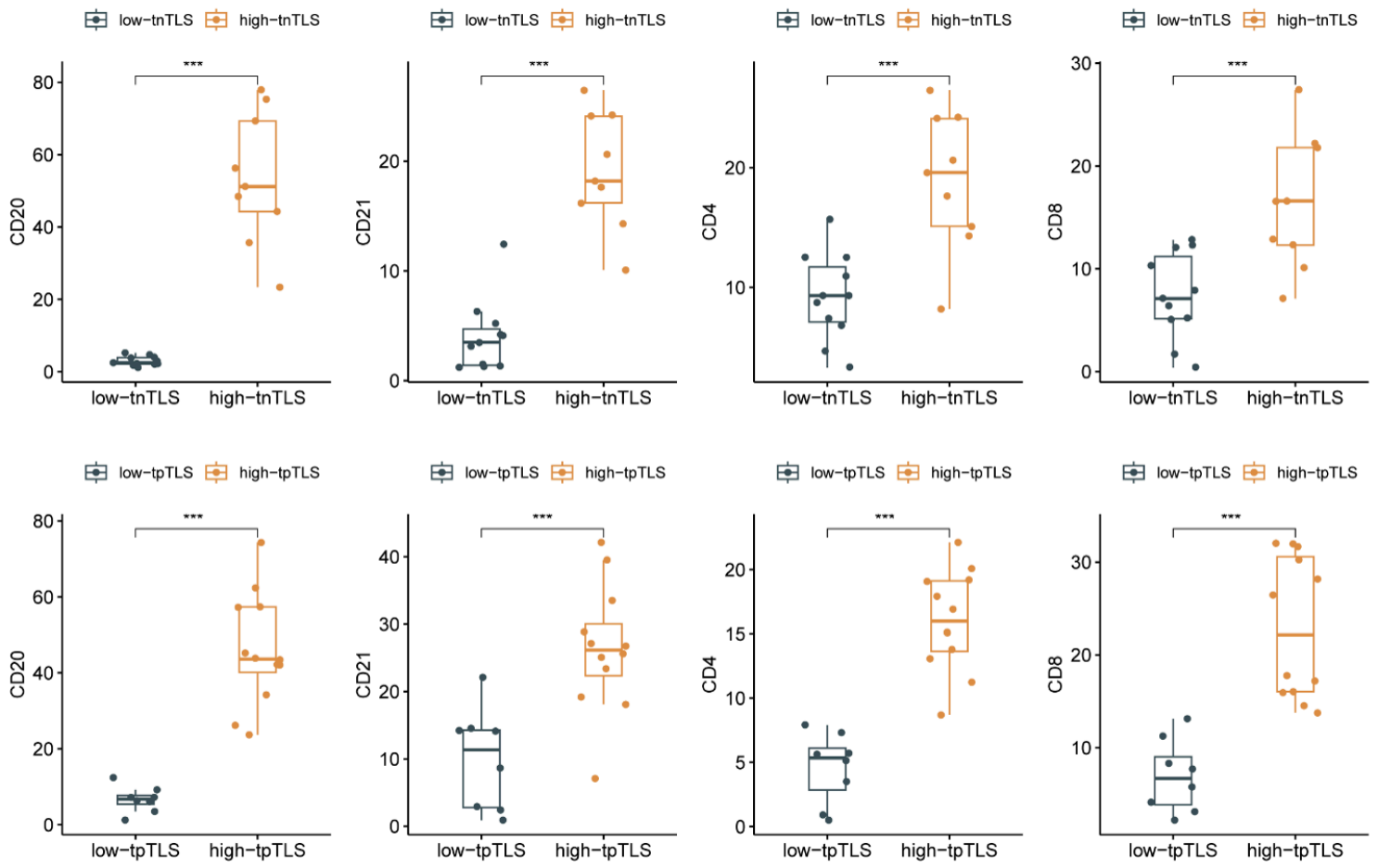


## Figure 4

Evaluation of tertiary lymphoid structures (TLSs) using multiplex immunofluorescence in PSCC patients. Composition of CD20, CD21, CD4, and CD8 cells subsets in low-tnTLS, high-tnTLS, low-tpTLS, and high-tpTLS groups. Comparisons were made using the Mann-Whitney U test. (** $P < .01$, ***$P < .001$)

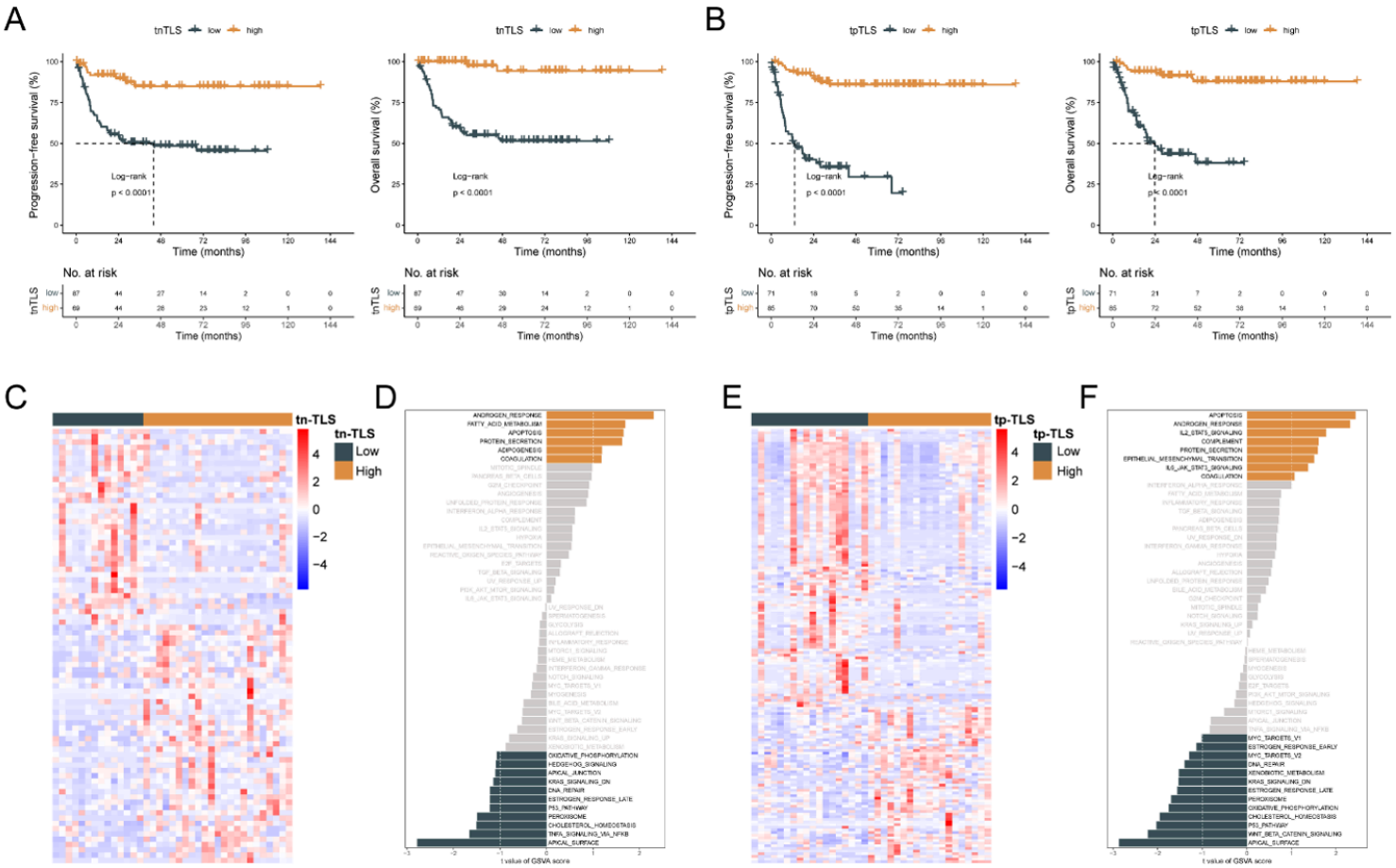


**Figure 5**

Prognostic value and discrepancy of tnTLS and tpTLS in PSCC. Kaplan-Meier curves showing progression-free survival (PFS) and overall survival (OS) of PSCC patients stratified by tnTLS (A) and tpTLS (B) in Cohort 1, respectively. Difference analysis of low-tnTLS and high-tnTLS in PSCC. Heatmap of DEGs between samples in PSCC with low-tnTLS and high-tnTLS group (C); Functional enrichment analysis of low-tnTLS and high-tnTLS group in PSCC (D). Difference analysis of low-tpTLS and high-tpTLS in PSCC. Heatmap of DEGs between samples in PSCC with low-tpTLS and high-tpTLS group (E); Functional enrichment analysis of low-tpTLS and high-tpTLS group in PSCC (F).

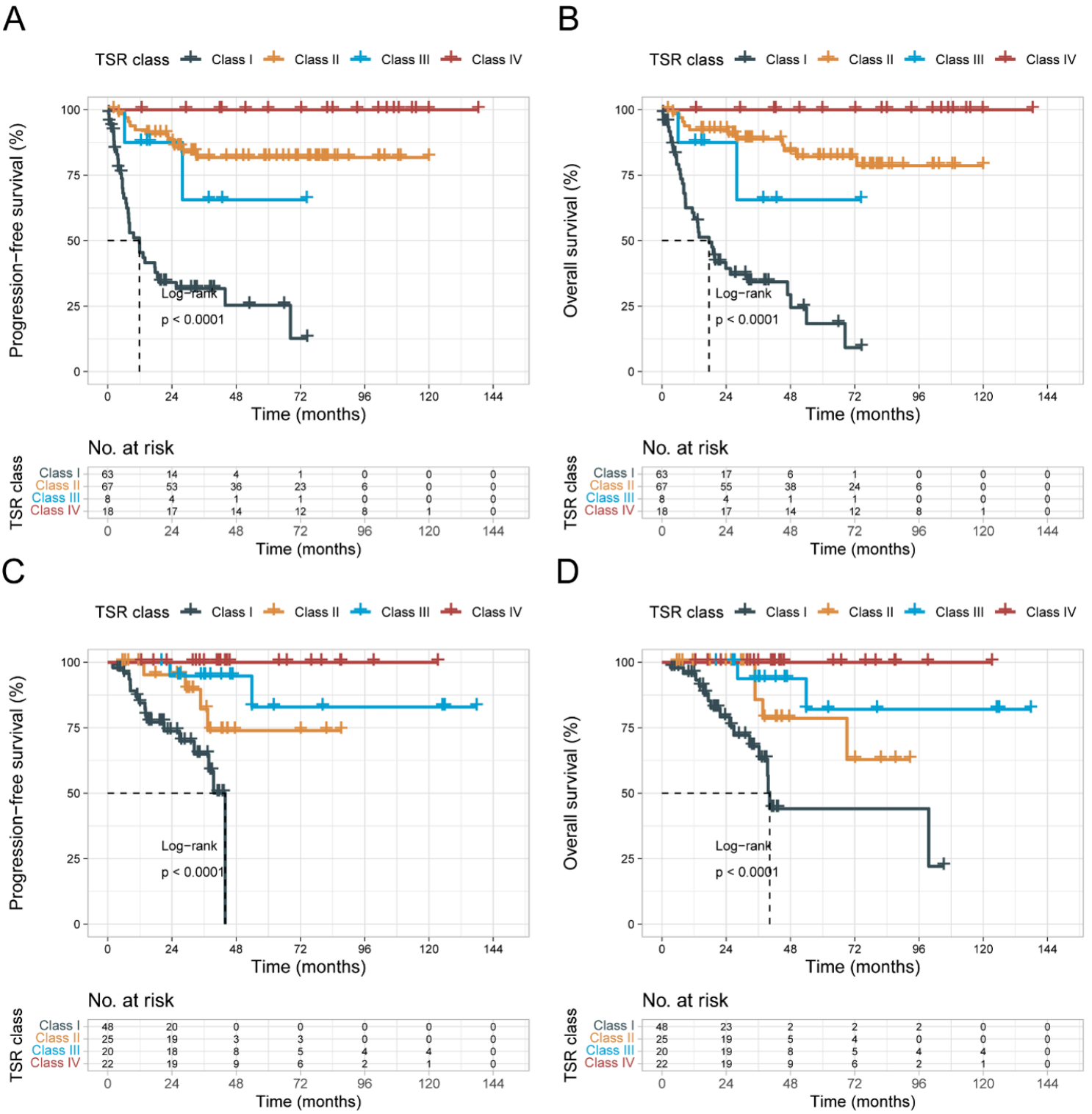


**Figure 6**

Prognostic value of TSR class in PSCC. Kaplan-Meier curves showing progression-free survival (PFS) and overall survival (OS) of PSCC patients with different TSR classes in cohort 1(A, B) and cohort 2 (C, D), respectively.

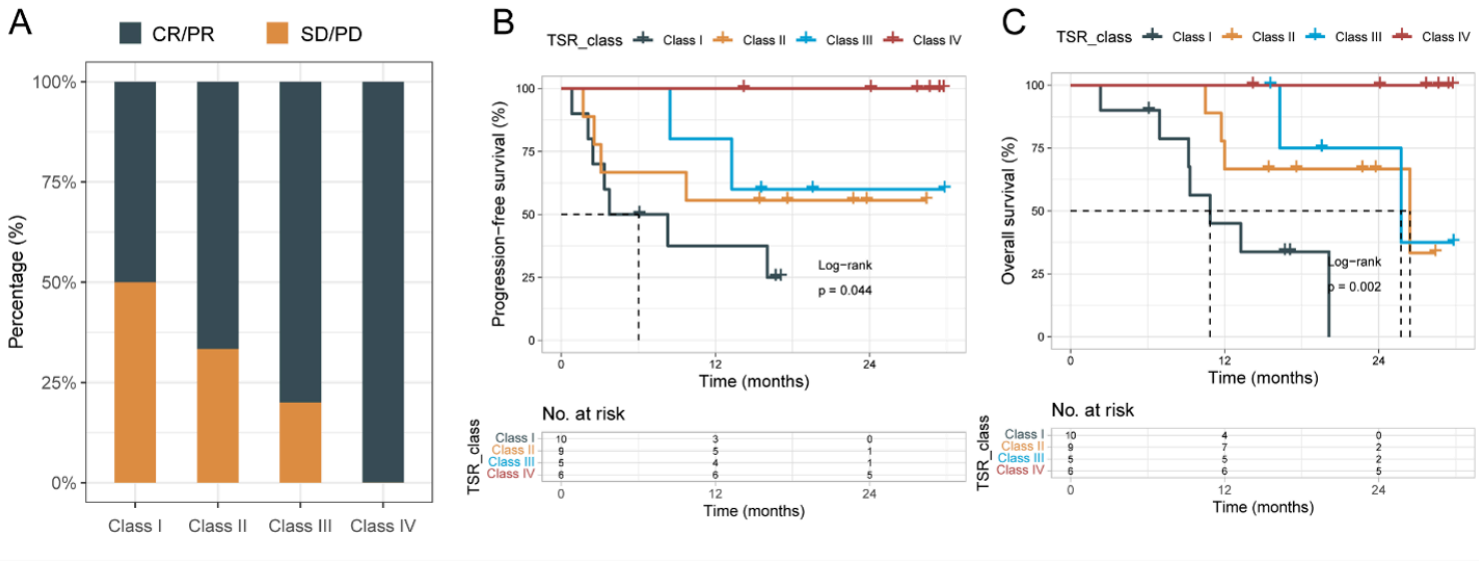


**Figure 7**

The prognostic meaning of TSR class in patients who received immunotherapy. The immunotherapy response in different TSR classes (A). Prognostic value of TSR class in PSCC received immunotherapy. Kaplan-Meier curves showing progression-free survival (PFS) (B) and overall survival (OS) (C) of PSCC patients with different TSR classes, respectively.

## Supplementary Files

This is a list of supplementary files associated with this preprint. Click to download.

- Tables.docx